Proceedings of ASME FEDSM'03
4th ASME_JSME Joint Fluids Engineering Conference
Honolulu, Hawaii, USA, July 6-10, 2003

FEDSM2003-45002

OBSERVATIONS OF CHAIN-REACTION BEHAVIOR AT BUBBLE COLLAPSE USING ULTRA HIGH SPEED VIDEO CAMERA

Keiichi Sato, Shigemasa Shimojo and Jun Watanabe
Department of Mechanical Engineering
Kanazawa Institute of Technology
Ishikawa, Japan

ABSTRACT

Collapsing behavior of cavitation bubbles is a very short phenomenon. In this study a new ultra-high-speed video camera with the maximum frame speed of 10^6 fps is used to observe the detailed aspects of three cavitation patterns such as separated vortex cavitation in a convergent-divergent channel, Karman-vortex-like cavitation in the wake flow of a circular cylinder and vibratory cavitation in an ultrasonic vibratory apparatus.

For a convergent-divergent channel, the re-entrant motion within the separation zone was observed together with bubble collapse in the divergent part. It was found that minute bubbles collapsed in a chain-reaction manner inside the separated zone with the re-entrant motion after the shedding of cavitation cloud.

For the wake flow of a circular cylinder, a collapsing motion of cavitation was observed as an axial-collapse type. The successive bubble collapses after the collapse of main bubble were caused due to pressure wave near the flow field.

For cavitation in a vibratory apparatus, cavitation bubbles on the vibratory disk surface were examined in detail, especially from the viewpoint of a non-cavitation ring. The disappearance of bubbles spread radially toward the outer region through the motion of vibratory horn.

Keywords: Cavitation, Bubble Collapse, Chain-Reaction, Collapse propagation, High-speed-Video Observation

INTRODUCTION

A cavitation bubble which occurs in a high-speed liquid flow shows a very high-speed behavior at its collapse. For a long time the growth or collapse phenomena of cavitation bubbles have been observed as a typical subject of high-speed photography [1]. On the other hand, recent developments of high speed video camera, namely new developments of solid-state image sensor can capture rapid moving images at (1,000,000 frames/s) 1Mfps [2, 3] and bring about further progress in cavitation studies. In the present study various kinds of cavitation phenomena were investigated by an ultra-high-speed video camera with an in-situ storage image sensor developed by Etoh et al. [3].

Most cavitation patterns behave in a complex manner as a cloud of cavitation. For example, a kind of attached cavitation such as sheet cavitation shows an unsteady motion as cloud cavitation with some regularity [4]. Cavitation bubbles produce high impact closely related to severe erosion through the rapid deformation of cavitation bubbles or cavitation clouds when the cavitation clouds are exposed to strong pressure fluctuation with some periodicity. The typical examples of high-impact-prone cavitations are as follows; (1) Karman-vortex-like cavitation in the wake of a circular or a triangular cylinder [e.g., 5], (2) cloud cavitation in a convergent-divergent channel or on a hydrofoil [e.g., 6], (3) vibratory cavitation in a cavitation erosion apparatus [e.g., 7, 8] and (4) cavitating water jet with periodic discontinuity [e.g., 9].

It seems to be no doubt that the high-speed interaction within the cavitation cloud makes a crucial role on the occurrence of high impact [10]. Filed, et al. [11, 12] made clear through a series of their investigations that the shock waves and micro-jets produce a chain reaction of bubble collapses by the observation of cavity behaviors in gelatin layer. Matsumoto and Shimada [13] showed by numerical simulation that a cloud of bubbles can locally produce high pressure inside of it. The recent result by Yagi et al. [14] is interesting from a practical viewpoint because they showed experimentally that the downstream collapse of bubbles can generate the upstream erosion in a long orifice for pressure reduction in a flow system.

The recent progress of a CCD image sensor has made possible the high-speed observation of cavitation bubbles with little difficulty. In the present experiment the picture capturing is made in various kinds of cavitating flows using two high-speed video cameras with the framing rate of 9 Kfps to 500Kfps. The propagation of bubble collapse is mainly examined for these unsteady cavitation phenomena.

EXPERIMENTAL APPARATUS AND PREVIOUS INVESTIGATIONS

Two kinds of high-speed video cameras were used to observe cavitation bubbles. The video-A with a maximum framing rate of 40.5Kfps (Kodak, EXTAPRO Model 4540) had been used in many cavitation experiments [15]. The video-B, an ultra-high speed camera, was a new one with a maximum rate of 1Mfps [3]. One or two metal halide lamps (150W; Photoron, HVC-SL) were used for continuous illumination. An accelerometer (TEAC, 501FS/FB) installed on the test section, in some cases, was used to make a trigger signal to synchronize the capture of video frame with the cavitation impact [15].

The cavitation experiment was conducted using three kinds of cavitation apparatus. The first and the second one were installed in a small closed type of cavitation tunnel [16] with a rectangular test section of 80 mm x 60 mm. They were a convergent-divergent channel shown in Fig.1 and a circular cylinder in Fig.2, respectively. The third one was a vibratory apparatus shown in Fig.3.

In the convergent-divergent channel, a separated-vortex type of cavitation occurred and appeared to be an unsteady attached-type cavitation with a periodic shedding of cavitation clouds [17]. The thickness of separated zone behind the convergent throat was relatively large. At the earlier stage of cavitation development, small-size vortex cavities occurred on the separated shear layer and after the coalescence of several stages grew to a large cavitation cloud which was finally shed downstream [6, 18]. The cavitation cloud shed downstream, after the strong collapse, showed a re-entrant motion toward the upstream direction in the separated zone.

The next observation was made for the cavitating flow behind a circular cylinder installed vertically in the test section as shown in Fig.2. The circular cylinder was positioned in a middle part of the test section. The Karman-vortex-like cavitation shed downstream as a cavitation cloud moved downstream in the wake of the circular cylinder with a rotating motion about the axis of vortex cavity. At a certain downstream position the long vortex cavities collapsed in an impinging manner toward the solid wall of the test section along the rotational axis of vortex cavitation [15, 19].

The third apparatus shown in Fig. 3 was a vibratory one which was often used as a typical cavitation erosion test apparatus [7]. The cavitation observation in the apparatus was mainly limited to a single instantaneous photography [8] or a high-speed photography with special illumination or attendant devices [20], because this erosion apparatus usually had a very high frequency such as 20KHz. However, recently, the videography with a framing rate higher than 20Kfps could observe such fast phenomena with little difficulty.

In the present study the bubble observations of high-speed interaction phenomena in three kinds of flow fields are examined on the basis of the results obtained by the high-speed videography with a high framing rate of 9K to 200Kfps.

EXPERIMENTAL RESULTS AND DISCUSSION

Bubble collapse of unsteady cavitation in convergent -divergent channel

The convergent-divergent channel is well known as a typical flow field with cloud cavitation [17]. Figure 4 shows the aspect of separated cavitation caused in the divergent part of the nozzle with high-speed video camera. The video framing rate is Fs=9Kfps. The region with high bubble density is depicted as a silhouette image. This type of cavitation sheds cavitation clouds downstream with a cyclic motion. After the shedding of cavitation cloud a reentrant motion is caused from the downstream to the upstream side inside the separated area.

Figure 4(a) shows the silhouette tracks of bubbling area collapsing one after another by the reentrant motion. In the present measurement an accelerometer is installed on the outer wall at the nozzle throat. The Frame of No.0 in Fig. 4(a) corresponds to that at the time when the bubble collapse due to the reentrant motion arrives at the leading part of the whole separated area, namely at the nozzle throat. After the arrival the formation of a new vortex cavity is made on the separated shear layer as shown in Frame No. 0 to 30. Next the vortex cavities cause several coalescences with each other to develop a large cavitation cloud.

Figure 4(b) shows the movement of reentrant motion obtained from the pictures in Fig. 4(a). The translational length is measured from the nozzle throat to the silhouette boundary which means the rapid change of bubble density and is depicted as a triangular plot under each picture of Fig. 4(a). The averaged translational velocity of re-entrant motion, as the

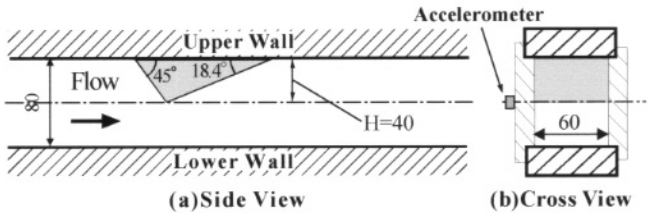

Fig.1 Flow field in a convergent-divergent channel

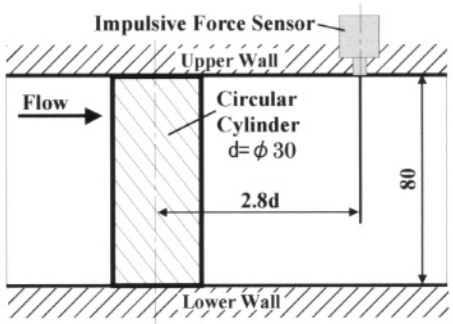

Fig.2 Flow field around a circular-cylinder

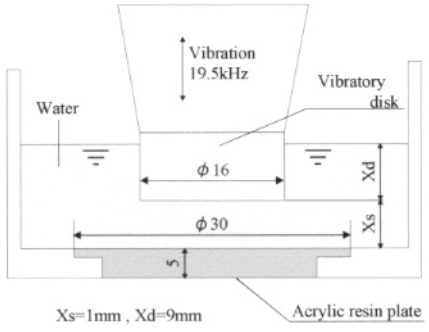

Fig.3 Flow field in a vibratory apparatus

result, can be approximately estimated to be Vp =10m/s.

Figure 5 shows the final aspect of the reentrant motion in the convergent-divergent channel, especially near the nozzle throat, using the ultra-high-speed video camera (Fs=100Kfps) to observe the behavior in detail. In this case the triggered observation is not made. Figure 5(a) indicates the detailed collapsing aspects of relatively large cavities near the leading part of the separated area (Frame No.15 to 73). In the first stage the bubble No.1 collapses (Frame No.15 to 35), in the second stage a cluster of bubbles No.2 collapse (Frame No.30 to 45), in the third stage the bubble No.3 collapses (Frame No. 45 to 60) and in the final stage the bubble No.4 collapses at the leading part (Frame No.60 to 73). It is confirmed from the results that a cluster of bubbles or a single bubble disappears one after another in a chain-reaction manner under the propagation of collapse at the final step of the reentrant motion.

Figure 5(b) shows the position of bubble edge to estimate the propagation velocity Vp of bubble collapses. The measurement position is depicted as a triangular plot under each picture of Fig. 5(a). The velocity around Frame No.30 to 68 is approximately estimated to be Vp=31m/s though the value around final collapsing point (Frame No.73) may be higher. The value is about 3 times as large as the average value indicated in Fig. 4(b).

The rebound phenomenon after the final collapse can be clearly observed in Frame No. 73 to 85. We can observe that a vortex cavity is formed in a singular manner such as rushing out into the main stream from the leading edge of separated

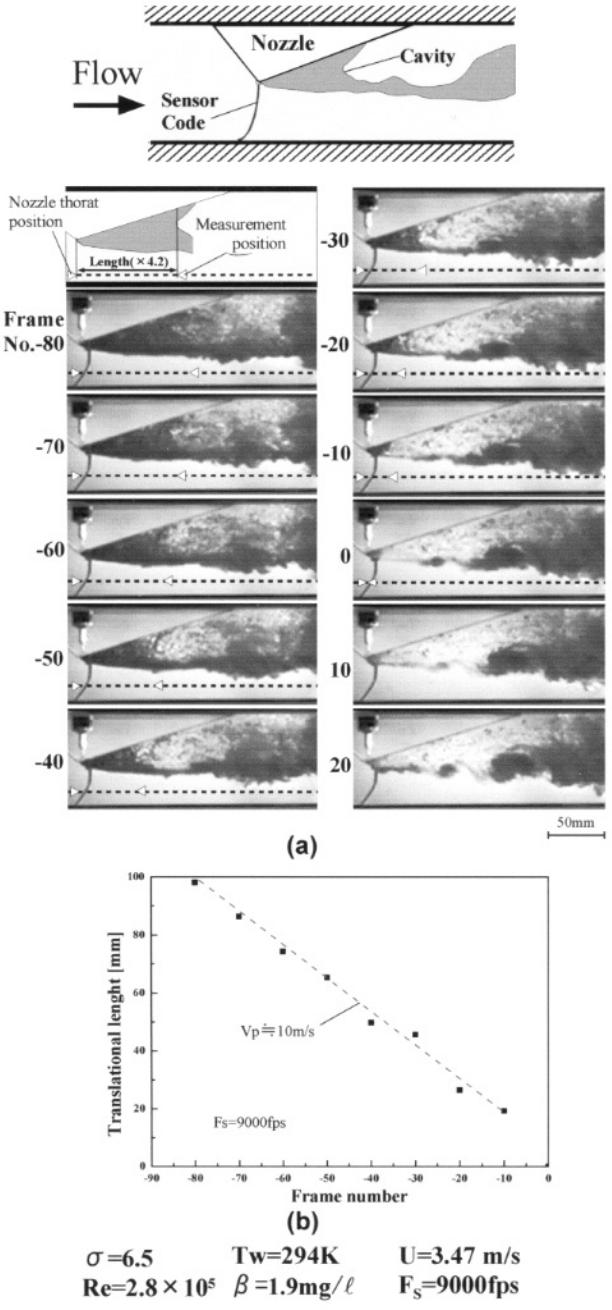

σ=6.5 Tw=294K U=3.47 m/s
Re=2.8×10^5 β=1.9mg/ℓ F_S=9000fps

Fig.4 Aspect of reentrant motion and collapse propagation velocity

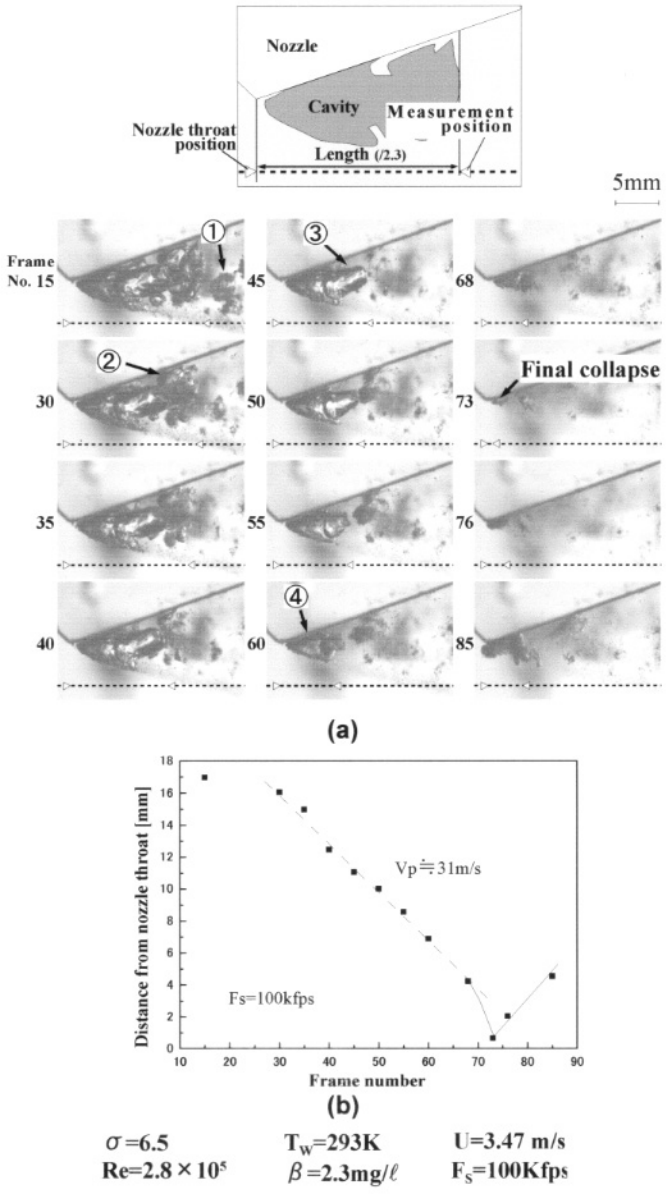

σ=6.5 T_W=293K U=3.47 m/s
Re=2.8×10^5 β=2.3mg/ℓ F_S=100Kfps

Fig.5 Aspect of chain-reaction collapse of bubbles and collapse propagation velocity

flow zone. The bubbles near the final stage appear to be very fast in the deformation and divided into minute bubbles.

After the final collapse (the arrival at the leading part) the formation of new vortex cavity begins on the separated shear layer as shown in Fig. 4(a) ; Frame No.0 to 20 or Fig. 5(a); Frame No.73 to 85. Figure 6 shows a characteristic aspect of vortex cavities on the shear layer observed at high framing rate of Fs=100Kfps. It is found that two vortex cavities consist of many minute bubbles respectively, move downstream at a translational velocity different from each other and are followed by a minute streamwise vortex cavity. Next the vortex cavities cause some growth and coalescence with each other to develop a large cavitation cloud.

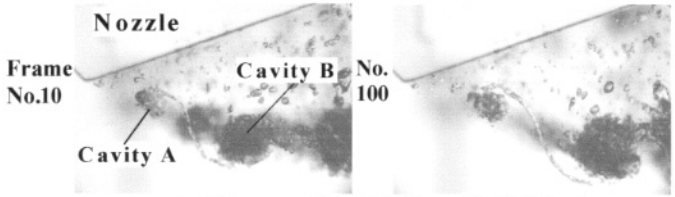

Fig.6 Vortex cavities on separated shear layer

Bubble collapse of separated vortex cavitation in a wake flow behind a circular cylinder

Separated vortex cavitation with an alternate shedding in a similar manner to the Karman vortex occurs in the wake of a two-dimensional circular cylinder. Figure 7 shows a whole aspect of vortex cavitation shed downstream from a viewpoint of the cylinder-span direction. It is found from the pictures that the vortex cavity is shed downstream with relatively high two-dimensionality at the initial stage though the aspect ratio Ar=8/3 of the cylinder is not very large.

First, the large vortex cavity shed downstream is divided into sub-cavities in the middle section of the flow channel [5]. Next, the sub-cavity positioned near the channel wall begins to collapse toward the wall along the rotating axis of vortex. It is known that the collapsing pattern can be classified into three types [5]. For the axial collapse type [5, 19], the cavity keeps the wall-side edge of it on the wall surface with shrinking the other edge as shown in Figs. 7 and 8. Figure 8, especially, shows the final collapsing step with the ultra-high speed video camera (Fs=500Kfps). The vortex cavity moves and shrinks toward the channel wall (Frame No. 0 to No.48) and then shifts to a rebounding motion. The averaged collapsing velocity is approximately estimated to be 48m/s around Frame No. 0 to 48 and is expected to be much higher at the final collapse point.

After the collapse of the main cavity the pressure wave caused at the collapse and rebound seems to be propagating through the surrounding water. In the case of Fig. 8, the bubbles A and B should be paid attention. The averaged propagation time from the collapse of main cavity (Frame No. 48) to that of the bubbles was measured to estimate the collapse propagation velocity though both bubbles begin to deform at an earlier stage. For the bubble-A the collapse occurs around Frame No.68 and then shifts to a rebounding motion. Therefore, the propagation velocity of collapse is about Fp=180m/s. For the bubble-B, the collapsing frame corresponds to Frame No.82. The velocity of about 190m/s is almost the same with that of the bubble-B. It should be noted that the propagation velocity

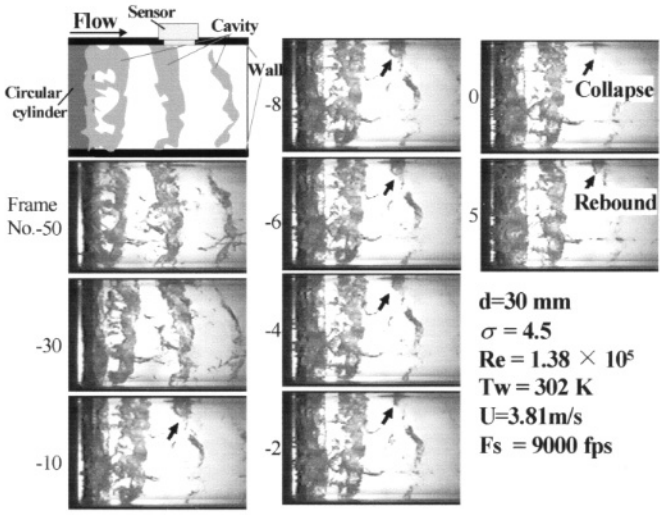

Fig.7 Cavity shedding and collapsing behaviors in the wake of a circular cylinder

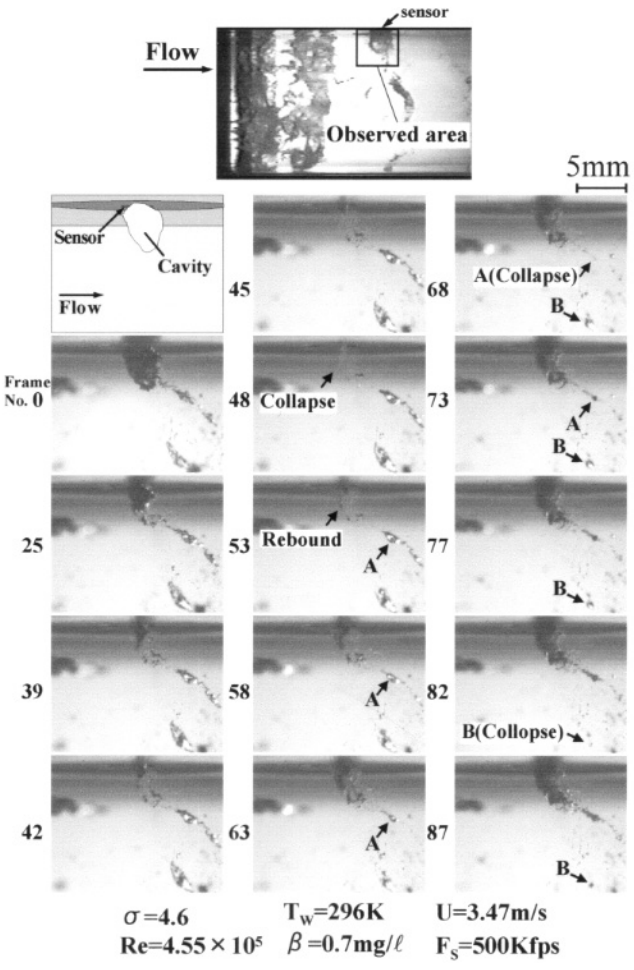

Fig.8 Cavity collapse near solid wall and propagation of bubble collapse

of collapse is not exactly equal to that of pressure wave because of the time delay due to the response time of bubble.

Bubble collapse of vibratory cavitation in the vibratory cavitation erosion apparatus

It is well known that the vibratory apparatus [7] for cavitation erosion test generates very high cavitation impacts. In the present study the aspect of cavitation bubbles is examined using the high-speed videography on the surface of vibratory horn (circular disk). The frequency of oscillation is 19.5KHz. The peak-to-peak amplitude of the horn displacement is 50μm.

Figure 9 shows typical instantaneous pictures of cavitation bubbles on the disk surface with flush period of 0.8μs. Figure 9(f) depicts the phase curve of the displacement in the vibratory horn. The picture in Fig. 9(b) corresponds to that at the highest position of the vibratory horn while the picture in Fig. 9(d) corresponds to that at the lowest position of the horn. The bubble appearance corresponds to the black area in the pictures. It is found that the bubble aspect shows a large change with the difference of vibratory horn displacement. It is, especially, pointed out that there are non-cavitating circular areas except for a small bubble in the center of them. These ring-shaped or circular areas have been called a shock-ring by Oba et. al [8, 9] or a non-cavitation circle in the present paper.

Figure 10 shows a typical example of ultra-high-speed observation with a framing rate of Fs=200Kfps. It means that about 10 pictures per a cycle can be taken because the vibration frequency is 19.5 KHz. The non-cavitation circle is shown by a dotted circle in Fig. 10(a) where it occurs and grows to large scale through the collapses of surrounding bubbles. Figure 10(b) shows the variation in the diameter of non-cavitation circle to estimate the propagation velocity of the circle from the approximate circle depicted in Fig. 10(a). The velocity is about 28 to 72 m/s as shown in Fig. 10(b). The velocity in this case is also very small compared with the acoustic speed (about 1500 m/s) in water.

On the other hand, Sanada et al. [20] indicated the value of about 1500 m/s as the propagation velocity of shock wave for vibratory cavitation on the vibratory erosion apparatus using a holographic interferometer. The difference of the velocities may be caused from various sources. The present result, for example, is obtained from the observation on the disk surface while the result of Sanada was from the free space over the disk surface. The density of bubbles, namely the void ratio is much

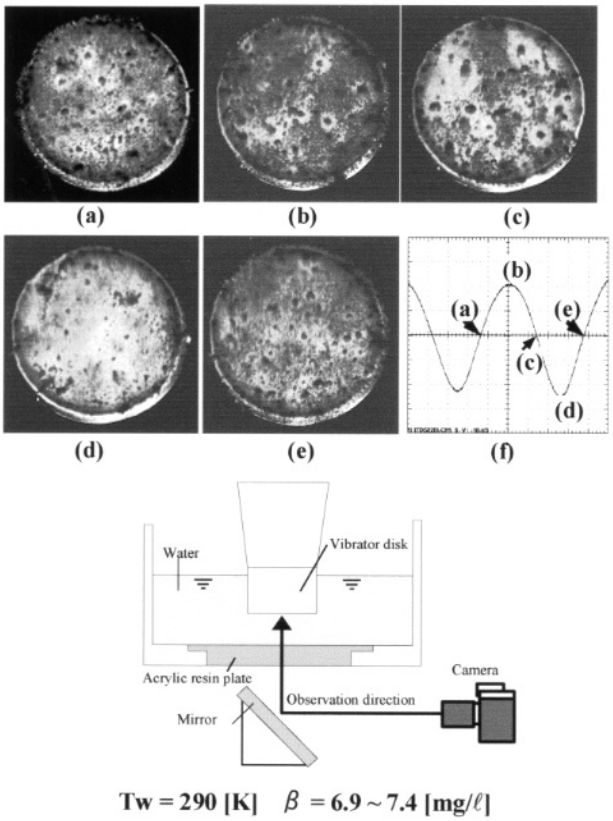

Fig.9 Appearance of bubbles on vibratory disk surface

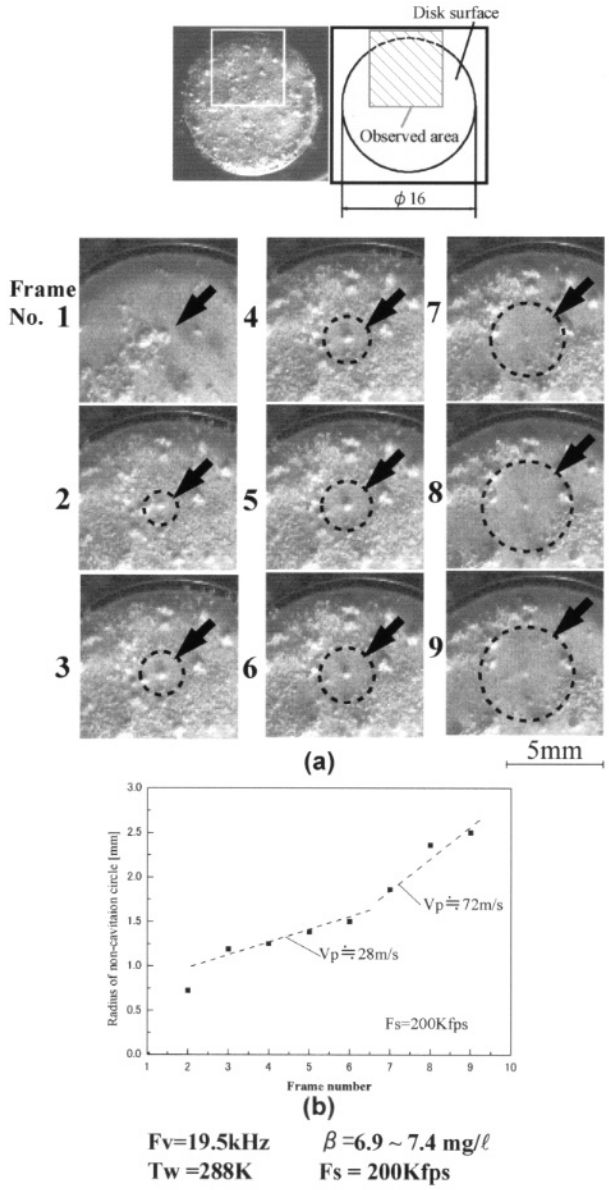

Fig.10 Behavior of non-cavitation circle on vibratory disk surface and propagation velocity

different from each other. According to the theory of gas-liquid two-phase flow, the acoustic propagation speed is reduced to be on the order of 10 m/s by only a small percentage of the void ratio [e.g., 21, 22]. The velocity of 28 to 72 m/s is appropriate for the value inside the cavitation clouds with many cavitation bubbles.

CONCLUSION

Various types of cavitation collapse were experimentally examined using a high-speed video camera with a framing rate of 9Kfps to 500Kfps from a main viewpoint of the propagation of bubble collapse. A new video camera with a maximum framing rate of 1Mfps used in the present study can bring about further progress in cavitation studies. The main results are summarized as follows.

(1) The reentrant motion was observed in a convergent-divergent channel for separated cavitation with the shedding of cavitation clouds.

In the separated cavitating zone the collapse propagation of a bubble cluster and/or a single bubble can be caused in a chain-reaction manner toward the leading part of cavitating zone from the downstream side.

(2) The cloud cavitation of Karman-vortex-type shed downstream from a circular cylinder can cause an axial collapse toward the channel wall along the rotating axis of vortex cavitation.

A slender cavity and/or a bubble-cluster show very fast contraction toward the channel wall. At the collapse of the cavity, the surrounding small bubbles are also collapsed by the pressure propagation due to the main bubble collapse.

(3) The detailed aspect of cavitation bubbles was observed on the disk surface vibrating at very fast speed. The dynamic behavior of non-cavitation circle was clearly captured on the disk surface.

The non-cavitation circle grows in the cavitating field at a certain velocity. The propagation velocity of the non-cavitation circle is much lower than the acoustic speed of pure water because the liquid state on the disk surface corresponds to the fact dominated by the cavitation clouds.

ACKNOWLEDMENT

The authors would like to thank Prof. G. Etoh and Dr. K. Takehara in Kinki University and Mr. Kondo in Shimadzu Corp. for the use of ultra-high-speed video camera. In addition the authors also thank Dr. Y. Saito for his earnest help on the videographic work.

REFERENCES

[1] Knapp, R.T., Daily, J.W. and Hammitt, F.G., 1970, Cavitation, pp. McGraw-Hill.

[2] Laberteaux, K.R., Ceccio, S.L. Mastrocola, V.J. and Lowrance, 1998, High Speed Digital Imaging of Cavitating Vortices, Experiments in Fluids, 24, pp. 489-498.

[3] Etoh, T.G., et al., 2002, A CCD Image Sensor of 1Mframes/s for Continuous Image Capturing of 103 Frames, 2002 Int. Solid-State Circuits Conf., 2.7, pp. 46-47.

[4] Franc, J.P., 2002, Partial Cavity Instabilities and Re-Entrant Jet, Proc. of the 4th Int. Symp. on Cavitation, Pasadena, Lecture.002, pp. 1-21.

[5] Sato, K., Sugimoto, Y. and Hoshino, K., 1998, Bubble Collapsing Behavior and Damage Pits of Separated Vortex Cavitation, Proceedings of Third International Symposium on Cavitation, Grenoble, pp. 157-162.

[6] Sato, K., Nakamura, H. and Saito, Y., 2001, Observations of Unsteady Separated-Type Cavitation in Convergent-Divergent Channel, Proc. of the 3rd Int. Symp. on Measurement Techniques for Multiphase Flows, Fukui, pp. 203-210.

[7] ASTM Designation, 1998, Standard Test Method for Cavitation Erosion Using Vibratory Apparatus, G32-98, pp. 107-120.

[8] Miyazaki, K., Ahmed, S.M. and Oba, R., 1993, High-Speed Observations of the Vibratory Cavitation Accompanying Hard Erosion, JSME Int. J., Ser.B, 36, pp. 511-516.

[9] Oba, R., 1994, The Severe Cavitation Erosion, Proc. of the Second Int. Symp. on Cavitation, Tokyo, pp. 1-8.

[10] Reisman, G.E., Wang, Y.-C. and Brennen, C.E., 1998, Observations of Shock Waves in Cloud Cavitation, J. Fluid Mech., 355, pp. 255-283.

[11] Dear, J.P. and Field, J.E., 1988, A Study of the Collapse of Arrays of Cavities, J. Fluid Mech., 190, pp. 409-425.

[12] Bourne, N.K. and Field J.E., 1992, Cavitation Damage by Bubbles Collapsed by Shock-Waves, Proc. IMechE, C453/046, pp. 49-54.

[13] Matsumoto, Y. and Shimada, 1997, Dynamics of Cavitation Bubble Cloud, ASME, FEDSM97-3267.

[14] Yagi, Y., Murase, M., Sato, K. and Hattori, S., 2003, Mechanism of Cavitation Erosion at the Exit of a Long Orifice, Proc. of the 4th ASME&JSME Joint Fluids Engineering Conference, Honolulu, to be published.

[15] Sato, K. and Ogawa, N., 1995, Collapsing Behavior of Vortex Cavitation Bubbles in the Wake of a Circular Cylinder, Cavitation and Gas-Liquid Flow in Fluid Machinery Devices, ASME, FED-226, pp. 119-125.

[16] Sato, K. and Kakutani, K., 1994, Measurement of Cavitation Inception, JSME International Journal, Ser.B, 37, pp. 306-312.

[17] Lush, P.A. and Skipp, S.R., 1986, High speed cine observations of cavitating flow in a duct, Int. J. Heat and Fluid Flow, 7-4, pp. 283-290.

[18] Sato, K., Saito, Y. and Nakamura, H., 2001, Self-Exciting Behavior of Cloud-like Cavitation and Micro-Vortex Cavities on the Shear Layer, Proc. of The First Int. Symp. on Advanced Fluid Information, Tohoku Univ., pp. 263-268.

[19] Dominguez-Cortazar, M.A., Franc, J.P. and Michel, J.M., 1997, The Erosive Axial Collapse of a Cavitating Vortex: An Experimental Study, Trans. ASME, J. Fluids Engng., 119, pp. 686-691.

[20] Sanada, N., Ikeuchi, J., Takayama, K. and Onodera, O., 1983, Generation and Propagation of Cavitation Induced Shock Waves in Ultrasonic Vibratory Testing, Proc. 14th Int. Symp. on Shock Tubes and Shock Waves, pp. 405.

[21] JSME, 1989, Handbook of Gas-Liquid Two-Phase Flow Technology, Corona Publishing Co. LTD., pp. 122-126.

[22] Hsieh, D.-Y. and Plesset, M.S., 1961, On the Propagation of Sound in a Liquid Containing Gas Bubbles, The Physics of Fluids, 4-8, pp. 970-975.